Parallel Structure General Repetitive Controller for General Grid-Connected PWM Converters

Wenzhou Lu[1*], Keliang Zhou[2], Ming Cheng[3], Jinfei Shen[1], Lei Wu[1]

[1] School of Internet of Things Engineering, Jiangnan University, Wuxi 214122, China
[2] School of Engineering, University of Glasgow, Glasgow G12 8QQ, Scotland, UK
[3] School of Electrical Engineering, Southeast University, Nanjing 210096, China
[*]luwenzhou@126.com

Abstract: This paper investigates parallel structure general repetitive control (PSGRC) and its error convergence rate by using exponential function properties. PSGRC offers a general repetitive control solution for power converters to mitigate power harmonics distortions. PSGRC with appropriate settings will lead to various RCs with various error convergence rates at interested harmonic frequencies, e.g. conventional RC (CRC), dual-model RC (DMRC), and odd harmonics RC (OHRC). As application examples, PSGRC was applied into general grid-connected pulse-width-modulation (PWM) converter systems. Experimental results show the effectiveness and advantages of PSGRC: three/single-phase grid-connected PWM converters can achieve zero-error current tracking and very fast current error convergence rate upon demand.

1. Introduction

Due to their high efficiency and controllability, power converters play a more and more important role in interfacing various generators and loads into electrical power systems [1]. However, power converter will induce power quality problems, e.g. harmonics distortion in the grid voltage/current [2-3]. To obtain "clean" interface, an accurate control solution is needed.

Based on internal model principle (IMP) [4], conventional repetitive controller (CRC) [5] can achieve steady-state zero-error tracking or disturbance elimination for any periodic signal with known fundamental period. In many practical applications, harmonic frequency components of a periodic signal to be tracked/eliminated usually concentrate at some specific harmonic frequencies. For example, for a single-phase off-grid PWM inverter [6-7], $4k\pm1$ (k=1,2,…) order harmonics (i.e. odd order harmonics) dominate the output voltage distortion. For a three-phase PWM rectifier [8], $6k\pm1$ (k=1,2,…) order harmonics dominate the feeding current distortion. If CRC is used in these converter applications, its dynamic response is relatively too slow to eliminate these specific harmonics effectively even if it can achieve zero-error current tracking performance. To solve this problem, researchers have proposed various RCs for various specific converter applications [6-7, 9-13], such as DMRC [6-7] and OHRC [9,11] for single-phase off-grid inverter, $6k\pm1$ RC [13] for three-phase off-grid inverter and so on. However, a general RC for various converters is not available until [14-15] proposed a parallel structure repetitive control (PSRC), which employs a series of paralleled $nk+i$ (i=0,1,2,..,n-1) order harmonic internal models.

PSRC with appropriate settings can achieve the zero-error tracking or disturbance elimination for all harmonics and has faster error convergence rate without losing tracking accuracy compared with CRC.

This paper will investigate the parallel structure based general RC (PSGRC) and its error convergence rate property in detail. PSGRC is proposed as a general controller for general grid-connected PWM converter systems. Case studies on PSGRC controlled grid-connected PWM converters are carried out to verify effectiveness and advantages of PSGRC.

2. PSGRC

2.1. PSGRC

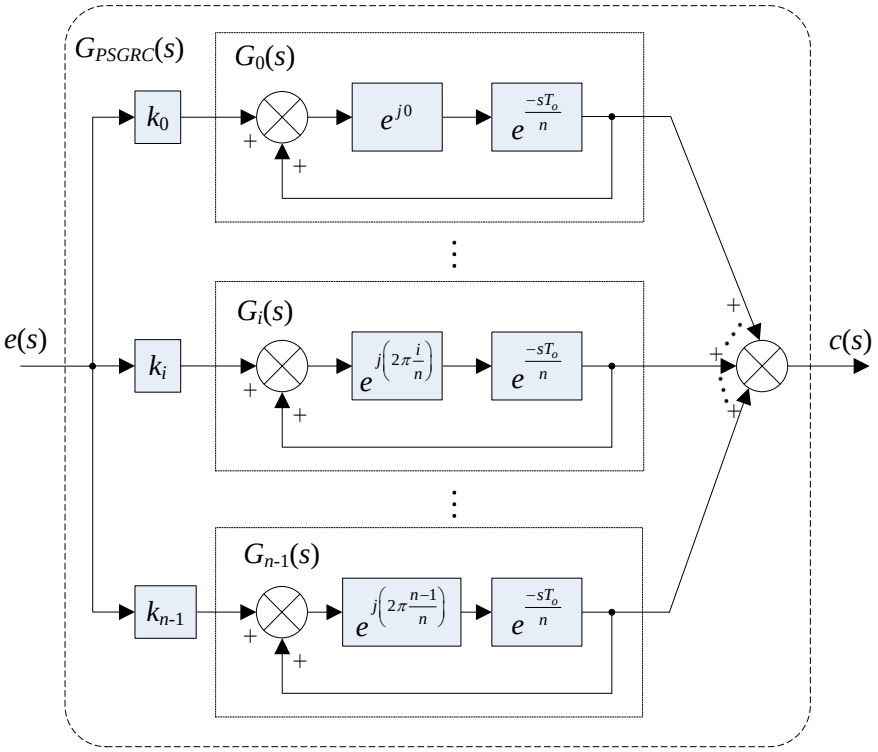

Fig. 1. *Parallel structure general repetitive control (PSGRC)*

Fig. 1 shows the parallel structure based general RC (PSGRC) [14-15], whose transfer function is:

$$G_{PSGRC}(s)=\sum_{i=0}^{n-1}\left[k_iG_i(s)\right]=\sum_{i=0}^{n-1}\left[k_i\frac{e^{j(i\cdot 2\pi/n)}}{e^{sT_o/n}-e^{j(i\cdot 2\pi/n)}}\right] \tag{1}$$

where, k_i is the control gain of the $nk+i$-th harmonic internal model (IM) $G_i(s)$ (i=0,1,…,n-1); n is integral and $n\geq 0$; $T_o= 2\pi/\omega_o=1/f_o$ is the fundamental period of signals with f_o being the fundamental frequency, ω_o being the fundamental angular frequency. From Eq. (1) and Fig. 1, it can be seen that PSGRC offers a general RC structure, which can be flexibly converted to CRC, DMRC, OHRC and so on.

2.2. Equivalent CRC

From Eq. (1), when n=1, PSGRC becomes CRC [8]. That is, CRC is one special case of PSGRC. Fig. 2 shows the most used and applied RC, i.e. CRC, whose transfer function is

$$G_{CRC}(s)=\frac{k_{rc}\cdot e^{-sT_o}}{1-e^{-sT_o}} \tag{2}$$

where k_{rc} is the control gain.

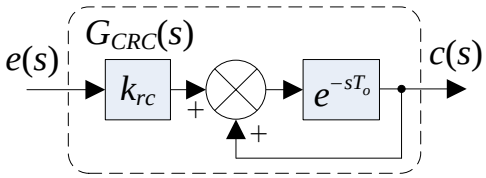

Fig. 2. *Conventional repetitive control (CRC)*

Moreover, from Eq. (1), when n>1, following Theorem shows that PSGRC is equivalent to CRC as some requirements being satisfied.

Theorem 1: If let $k_i=k_{rc}/n, i=0,1,2,\ldots,n-1$, then the proposed PSGRC controller is equivalent to CRC controller, *i.e.* the following equation is tenable:

$$G_{PSGRC}(s)=\frac{k_{rc}}{n}\sum_{i=0}^{n-1}\frac{e^{j(2\pi i/n)}}{e^{sT_o/n}-e^{j(2\pi i/n)}}=\frac{k_{rc}}{e^{sT_o}-1}=G_{CRC}(s) \tag{3}$$

Proof: When n=1, we can easily get that Eq. (3) is tenable; when n>1, let

$$x=e^{sT_o/n} \tag{4}$$

Thus, if following equation can be proved, Eq. (3) is tenable:

$$\frac{1}{n}\sum_{i=0}^{n-1}\frac{e^{j(2\pi i/n)}}{x-e^{j(2\pi i/n)}}=\frac{\left\{\sum_{p=0}^{n-1}\left[e^{j\frac{p\cdot 2\pi}{n}}\cdot\prod_{\substack{i=0\\ i\neq p}}^{n-1}\left(x-e^{j\frac{i\cdot 2\pi}{n}}\right)\right]\right\}/n}{\prod_{i=0}^{n-1}\left(x-e^{j(2\pi i/n)}\right)}=\frac{1}{x^n-1} \tag{5}$$

Because the roots of x^n-1=0 are $e^{j2\pi k/n}$ with k=0,1,…,n-1, we can obtain the following equation

$$x^n-1=\prod_{i=0}^{n-1}\left(x-e^{j(2\pi i/n)}\right) \tag{6}$$

Therefore, if the following equation can be proved, Eq. (5) is tenable.

$$\sum_{p=0}^{n-1}\left[e^{j\frac{p\cdot 2\pi}{n}}\cdot\prod_{\substack{i=0\\ i\neq p}}^{n-1}\left(x-e^{j\frac{i\cdot 2\pi}{n}}\right)\right]=n \tag{7}$$

Using the properties of exponential function

$$e^{j(2\pi i/n)}=e^{j\left[2\pi(i+nk)/n\right]} \tag{8}$$

where both n and k are integer.

Then, we can obtain the following equation

$$\sum_{p=0}^{n-1}\left[e^{j\frac{p\cdot 2\pi}{n}}\prod_{\substack{i=0\\ i\neq p}}^{n-1}\left(x-e^{j\frac{i\cdot 2\pi}{n}}\right)\right]=\sum_{p=0}^{n-1}\left[e^{j\frac{p\cdot 2\pi}{n}}\prod_{i=p+1}^{p+n-1}\left(x-e^{j\frac{i\cdot 2\pi}{n}}\right)\right] \tag{9}$$

Therefore, if the following equation can be proved, Eq. (7) is tenable.

$$\sum_{p=0}^{n-1}\left[e^{j\frac{p}{n}2\pi}\cdot\prod_{i=p+1}^{p+n-1}\left(x-e^{j\frac{i}{n}2\pi}\right)\right]=n \tag{10}$$

We have

$$\sum_{p=0}^{n-1}\left[e^{j\frac{p}{n}2\pi}\prod_{i=p+1}^{p+n-1}\left(x-e^{j\frac{i}{n}2\pi}\right)\right]=\sum_{i=1}^{n}\left[A_i x^{n-i}\sum_{q=0}^{n-1}\left(e^{j\frac{q}{n}2\pi}\right)^i\right] \tag{11}$$

where

$$\sum_{q=0}^{n-1}\left(e^{j\frac{q}{n}2\pi}\right)^i=\frac{e^{j(2\pi i)}-1}{e^{j(2\pi i/n)}-1} \tag{12}$$

When $i=n$, we can obtain

$$\sum_{q=0}^{n-1}\left(e^{j\frac{q}{n}2\pi}\right)^i\Bigg|_{i=n}=\frac{e^{j(i\cdot 2\pi)}-1}{e^{j(2\pi i/n)}-1}\Bigg|_{i=n}=\sum_{r=0}^{n-1}e^{j\left(\frac{r}{n}2\pi i\right)}\Bigg|_{i=n}=n\,; \tag{13}$$

when $0<i<n$ with i being integer, we can obtain

$$\sum_{q=0}^{n-1}\left(e^{j\frac{q}{n}2\pi}\right)^i\Bigg|_{\substack{0<i<n\\ i \text{ is integer}}}=\left[\frac{e^{j(i\cdot 2\pi)}-1}{e^{j(2\pi i/n)}-1}\right]_{\substack{0<i<n\\ i \text{ is integer}}}=0\,. \tag{14}$$

Therefore, in Eq. (11), all terms corresponding to A_i with $0<i<n$ with i being integer equal to zero and only the value of A_n is needed to calculate Eq. (11) as follows

$$A_n=(-1)^{n-1}e^{j\frac{1}{n}2\pi}e^{j\frac{2}{n}2\pi}\cdots e^{j\frac{n-1}{n}2\pi}=(-1)^{n-1}e^{j(n-1)\pi}=1 \tag{15}$$

So we can obtain

$$\sum_{p=0}^{n-1}\left[e^{j\frac{p}{n}2\pi}\prod_{i=p+1}^{p+n-1}\left(x-e^{j\frac{i}{n}2\pi}\right)\right]=A_n\sum_{q=0}^{n-1}\left(e^{j\frac{q}{n}2\pi}\right)^n=n \tag{16}$$

Thus, Eq. (10) is proved and then both Eq. (7) and (5) are proved. In the end, Eq. (3) is proved, i.e. Theorem 1 is proved.

2.3. Equivalent DMRC

From Eq. (1), when n=2, PSGRC becomes DMRC [6-7], shown in Fig. 3. That is, DMRC is also one special case of PSGRC. Its transfer function is

$$G_{DMRC}(s) = k_0 G_0 + k_1 G_1 = k_0 \frac{e^{-sT_o/2}}{1-e^{-sT_o/2}} + k_1 \frac{-e^{-sT_o/2}}{1+e^{-sT_o/2}} \tag{17}$$

where k_0 and k_1 are the control gains for even harmonics IM G_0, only effective for even harmonics, and odd harmonics IM G_1, only effective for odd harmonics, respectively.

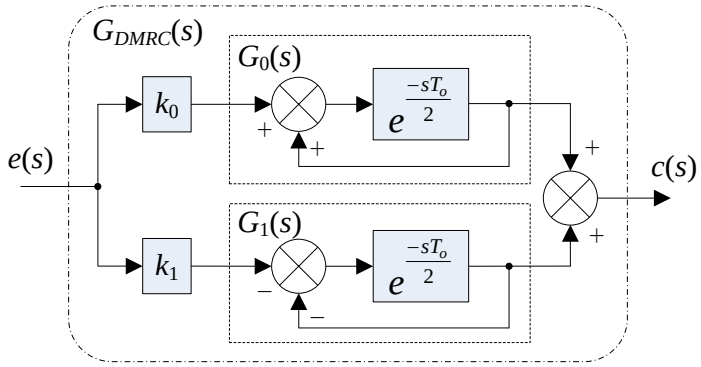

Fig. 3. *Dual-model repetitive control (DMRC)*

Obviously, using Theorem 1, when k_0=k_1, the DMRC shown in Eq. (17) is equivalent to a CRC with k_{rc}=2k_0=2k_1 in Eq.(2).

Especially, from Eq.(17), when k_0=0, k_1=k_{rc}, DMRC is equivalent to OHRC [9, 11], shown in Fig. 4. That is, OHRC is one special case of DMRC, or PSGRC. Its transfer function is

$$G_{OHRC}(s) = k_{rc} \cdot \frac{-e^{-sT_o/2}}{1+e^{-sT_o/2}} \tag{18}$$

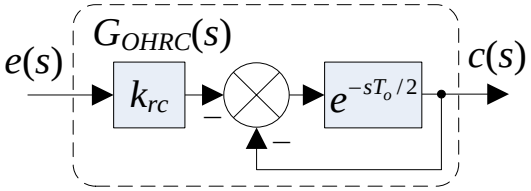

Fig.4 Odd-harmonic repetitive controller (OHRC)

Fig. 4. *Odd-harmonic repetitive controller (OHRC)*

It can be seen from Fig. 3-4 that DMRC is equivalent to the combination of one OHRC and one even-harmonics RC (EHRC) in parallel. The fundamental idea of DMRC is to categorize all harmonics into two groups, i.e. odd and even harmonics, controlled by parallel OHRC and EHRC respectively. The control gains k_0 and k_1 for OHRC and EHRC in DMRC can be tuned independently.

3. Error Convergence Rate Analysis Using Exponential Function Properties

3.1. Exponential function properties

In order to investigate the error convergence rate of various RCs, especially the PSGRC, using the following exponential function properties [16]:

$$\pi \frac{e^{\pi x} + e^{-\pi x}}{e^{\pi x} - e^{-\pi x}} = x \sum_{k=-\infty}^{+\infty} \frac{1}{x^2 + k^2} = \frac{1}{x} + \sum_{k=1}^{+\infty} \frac{2x}{x^2 + k^2} \tag{19}$$

we can get

$$\frac{1+e^{-2\pi x}}{1-e^{-2\pi x}}=\frac{e^{\pi x}+e^{-\pi x}}{e^{\pi x}-e^{-\pi x}}=\frac{1}{\pi x}+\frac{1}{\pi}\sum_{k=1}^{+\infty}\frac{2x}{x^2+k^2} \tag{20}$$

In Eq. (20), let $x=s/\omega_o$ and following equation can be achieved:

$$\frac{1+e^{-sT_o}}{1-e^{-sT_o}}=\frac{2}{T_o s}+\frac{2}{T_o}\sum_{k=1}^{+\infty}\frac{2s}{s^2+\left(k\omega_o\right)^2} \tag{21}$$

Then, we have

$$\frac{1}{1-e^{-sT_o}}=\frac{1}{2}\left(\frac{1+e^{-sT_o}}{1-e^{-sT_o}}\right)+\frac{1}{2}=\frac{1}{2}+\frac{1}{T_o}\left[\frac{1}{s}+\sum_{k=1}^{+\infty}\frac{2s}{s^2+\left(k\omega_o\right)^2}\right] \tag{22}$$

and

$$\frac{e^{-sT_o}}{1-e^{-sT_o}}=\frac{1+e^{-sT_o}}{1-e^{-sT_o}}-\frac{1}{1-e^{-sT_o}}=-\frac{1}{2}+\frac{1}{T_o}\left[\frac{1}{s}+\sum_{k=1}^{+\infty}\frac{2s}{s^2+\left(k\omega_o\right)^2}\right] \tag{23}$$

3.2. CRC

From Eq. (23), the CRC in Eq. (2) is equivalent to the sum of proportional (P), integral (I) and resonant (R) items shown in Fig.5. Its transfer function can be written as

$$G_{CRC-PIR}\left(s\right)=k_{rc}\cdot\left\{-\frac{1}{2}+\frac{1}{sT_o}+\sum_{k=1}^{+\infty}\frac{2s/T_o}{s^2+\left(k\omega_o\right)^2}\right\} \tag{24}$$

where the control gains for P, I and R are the same, i.e. k_{rc}, although the internal coefficients are different, i.e. -1/2 for P, $1/T_o$ for I, and $2/T_o$ for every R.

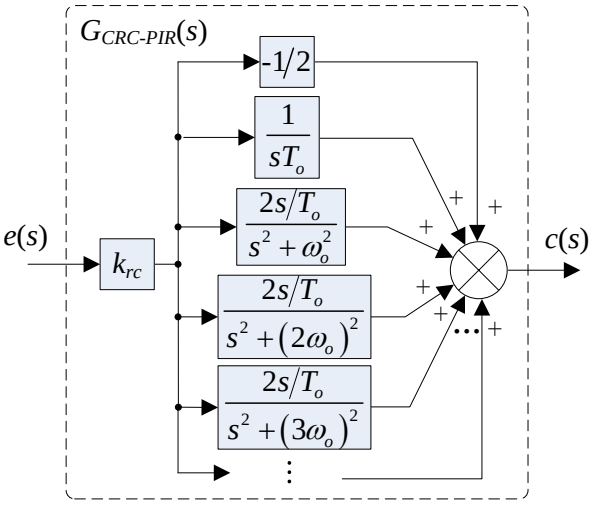

Fig. 5. *Equivalent parallel PIR format of CRC*

As we know, the error convergence rate of CRC is directly proportional to the control gain k_{rc}. The larger k_{rc} is, the faster the error convergence rate is. From (24) since identical control gain is assigned to all

harmonic frequencies, it is impossible to independently tune control gain for specific harmonics for optimizing the dynamic performance of CRC.

3.3. SHMRC

In practical, the harmonic spectrum is not even distributed. If large control gains are assigned to dominant harmonics, the tracking error convergence rate can be improved. That is to say, it is unnecessary to let all control gains in Fig. 5 to be identical value. Based on this idea, selective harmonics multiple resonant control (SHMRC) [17] shown in Fig. 6 can be achieved naturally, whose transfer function is

$$G_{SHMRC}(s) = k_P \cdot (-\frac{1}{2}) + k_I \cdot \frac{1}{sT_o} + \sum_{k=1}^{+\infty} \frac{k_{Ri} \cdot 2s/T_o}{s^2 + (k\omega_o)^2} \tag{25}$$

where control gains k_P, k_I and k_{Ri} (i=1,2,…) with different values can be assigned. Therefore, through independently and flexibly tuning the control gains in Eq. (25), error convergence rate can be improved, and "tailor-made" tracking or eliminating for harmonics can be achieved. In practical application, it is impossible and unnecessary to assign nonzero values to infinity terms in Eq. (25). However, there are still so many control gains to be tuned. It is not easy to optimize these control gains for a stable operation.

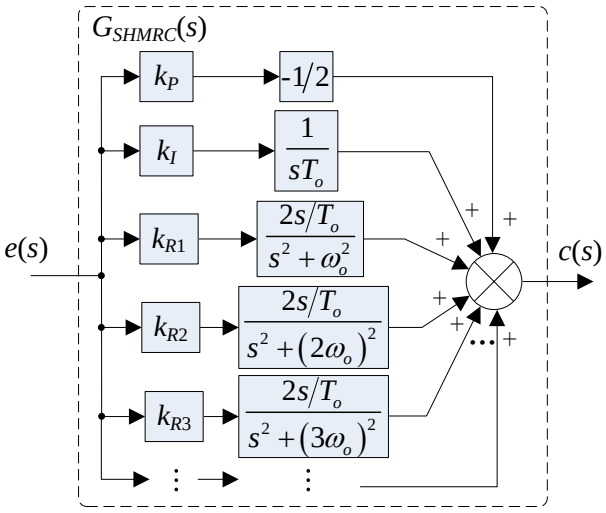

Fig. 6. *Selective harmonics multiple resonant controller(SHMRC)*

3.4. DMRC

Similarly to CRC in Eq. (24), using the properties of the exponential function, the equivalent parallel PIR format of DMRC can be achieved as follows

$$G_{DMRC-PIR}(s) = k_0 G_{0-PIR} + k_1 G_{1-PIR} \tag{26}$$

where

$$G_{0-PIR} = -\frac{1}{2} + \frac{2}{sT_o} + \sum_{k=1}^{+\infty} \frac{4s/T_o}{s^2 + (2k\omega_o)^2} \tag{27}$$

$$G_{1-PIR} = -\frac{1}{2} + \sum_{k=1}^{+\infty} \frac{4s/T_o}{s^2 + \left(\left[2k-1\right]\omega_o\right)^2} \tag{28}$$

When k_0=0, k_1=k_{rc}, DMRC is equivalent to OHRC. Thus, the equivalent parallel PIR format of OHRC can be derived in the similar way.

From Eq. (26)-(28) and (24), it can be seen that the internal coefficient of every odd/even-harmonic R for DMRC, i.e. $4/T_o$, is twice as large as that for CRC, i.e. $2/T_o$. Thus, compared with CRC, DMRC with same control gain can offer up to twice faster error convergence rate at most.

Therefore, through tuning the weighted coefficients k_i (i=0,1) independently in accordance with the odd- and even- harmonics distribution, DMRC can perfectly tracked or eliminated all harmonics at optimal total error convergence rate. For example, if odd harmonics dominate the distortion, letting k_1>k_0, DMRC can achieve the improved overall error convergence rate without reducing tracking accuracy.

3.5. PSGRC

Similarly, the equivalent PIR format for $G_i(s)$ (i=0,1,…,n-1) in PSGRC can be rewritten as:

$$G_{i-PIR}(s) = -\frac{1}{2} + \frac{n}{T_o\left(s - ji\omega_o\right)} + \sum_{k=1}^{+\infty} \frac{2n\left(s - ji\omega_o\right)/T_o}{\left(s - ji\omega_o\right)^2 + n^2k^2\omega_o^2} \tag{29}$$

From Eq. (29), the poles of $G_{i\text{-}PIR}(s)$ or $G_i(s)$ are located at $(\pm nk+i)\omega_o$, i=0,1,2,…,n-1, k=0,1,2,… . At these frequencies, the amplitude of $G_i(s)$ approaches infinity, and thus the $\pm nk+i$ th -harmonic components can be completely tracked or eliminated. Paralleled $nk+i$ th -harmonic internal model $G_i(s)$ (i=0,1,2,…,n-1) shown in Fig. 1 enable PSGRC to completely tracked or eliminated all these harmonics.

Moreover, control gain k_i (i=0,1,2,…,n-1) of PSGRC can be customized and independently tuned to optimize the total convergence rate. It can be seen from Eq. (29) that, the internal coefficient of $\pm nk+i$ th -harmonic terms, i.e. $2n/T_o$, is n times than that of CRC, i.e. $2/T_o$ in Eq. (24). Thus, with same control gain, the error convergence rate of PSGRC at $\pm nk+i$ th harmonic frequencies is n times faster than that of CRC. Therefore, through optimal tuning of these n control gains for $G_i(s)$ (i=0,1,2,…,n-1) in accordance with the harmonics distribution, the total error convergence rate of PSGRC would be faster than that of CRC. For example, if odd-harmonics are the dominant components, PSGRC with (k_1+k_3)>(k_0+k_2) can improve its overall error convergence rate without reducing its tracking accuracy.

4. General RC-controlled Grid-connected PWM Converter System

4.1. General Grid-connected PWM Converters

Fig. 7(a) and 7(b) show the general three-phase (3-P) and single-phase (1-P) grid-connected PWM converters. Both can work in the rectifier and inverter states.

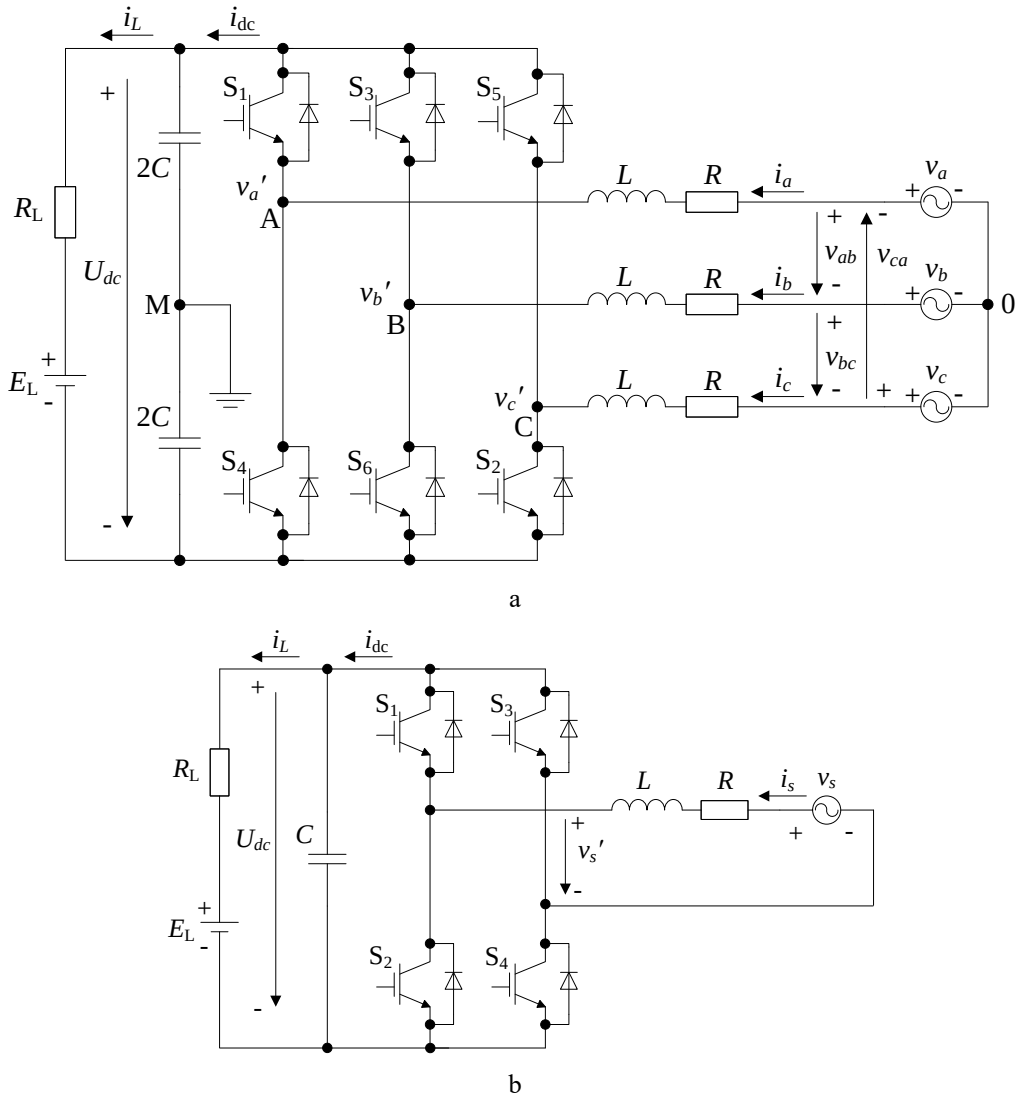

Fig. 7. *Grid-connected PWM converters*
a Three-phase (3-P)
b Single-phase (1-P)

In the rectifier state, the mathematics model can be described into

$$\dot{i}_j = -\frac{R}{L} i_j + \frac{1}{L}\left(v_j - v_j'\right) \text{ (} j\text{=}a,b,c \text{ for 3-P; } j\text{=}s \text{ for 1-P)} \tag{30}$$

and

$$\dot{U}_{dc} = -\frac{1}{CR_L} U_{dc} + \frac{1}{C} i_{dc} + \frac{1}{CR_L} E_L \text{ (for both 3-P \& 1-P)} \tag{31}$$

where C, L and R are the dc-side capacitor, ac-side inductance, and ac-side resistor, respectively; R_L is the resistor load, E_L is the inverse electromotive force; inductance currents i_a, i_b, i_c, i_s and dc-side capacitor voltage U_{dc} are the state variables; v_a, v_b, v_c are the a, b, c three-phase grid voltages; v_s is the single-phase grid voltage; i_{dc} is the dc output current; i_L is the dc load current; v_a', v_b', v_c' are the a, b, c three-phase PWM modulation voltages; v_s' is the single-phase PWM modulation voltage.

In the inverter state, the mathematics model is the same with Eq. (30). The dc voltage U_{dc} is assumed to be constant. PWM modulated voltages can be described by:

$$v_j(t) = \frac{1}{2} U_{dc}(t) s_j \ (j\text{=a,b,c for 3-P}) \tag{32}$$

and

$$v_s'(t) = U_{dc}(t) s_s \ (\text{for 1-P}) \tag{33}$$

DC output current can be written as:

$$i_{dc} = i_a s_a + i_b s_b + i_c s_c \ (\text{for 3-P}) \tag{34}$$

and

$$i_{dc} = i_s s_s \ (\text{for 1-P}) \tag{35}$$

where s_a, s_b, s_c and s_s are the switching functions of three-phase and single-phase bridges, defined as

$$s_j\,(j = a,b,c) = \begin{cases} +1, \text{ on for upper \& off for lower switches for } j \text{ phase} \\ -1, \text{ on for lower \& off for uper switches for } j \text{ phase} \end{cases} \tag{36}$$

and

$$s_s = \begin{cases} +1, \ \text{on for } S_1S_4 \ \text{\& off for } S_2S_3 \\ \text{-1}, \ \text{on for } S_2S_3 \ \text{\& off for } S_1S_4 \end{cases} \tag{37}$$

In the rectifier state, the control objective is to achieve unit power factor, high current tracking accuracy and constant output dc voltage. Output equations are:

$$\boldsymbol{y} = [i_a \quad i_b \quad i_c \quad U_{dc}]^T \ (\text{for 3-P}), \tag{38}$$

and

$$\boldsymbol{y} = [i_s \quad U_{dc}]^T \ (\text{for 1-P}), \tag{39}$$

respectively, where both DC voltage and AC current(s) need to be controlled.

In the inverter state, the control objective is to achieve adjustable power factor and high current tracking accuracy. Output equations are:

$$\boldsymbol{y} = [i_a \quad i_b \quad i_c]^T \ (\text{for 3-P}) \tag{40}$$

and

$$y = i_s \ (\text{for 1-P}) \tag{41}$$

respectively, where only AC current(s) need to be controlled.

4.2. General RC Control System

Fig. 8 shows the traditional closed-loop feedback control system with RC plugged into, where $G_{rc}(z)$ is the plug-in RC; $G_c(z)$ is the traditional feedback controller; $G_p(z)$ is the plant; $y(z)$ is the real output; $y_{ref}(z)$ is the reference input; $e(z)=y_{ref}(z)-y(z)$ is the tracking error and the input of $G_{rc}(z)$; $c(z)$ is the output of $G_{rc}(z)$; $u(z)$ is the output of $G_c(z)$; $d(z)$ is the external disturbance signal.

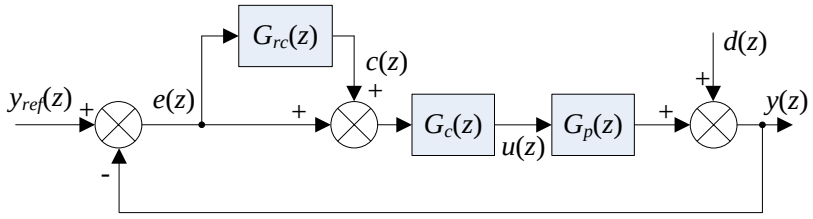

Fig. 8. *Structure of the plug-in repetitive control system*

The output $y(z)$ with plug-in RC is

$$\begin{aligned} y(z) &= G(z)\cdot y_{ref}(z) + G_d(z)\cdot d(z) \\ &= \frac{\left[1+G_{rc}(z)\right]H(z)}{1+G_{rc}(z)H(z)}\, y_{ref}(z) + \frac{\left[1+G_c(z)G_p(z)\right]^{-1}}{1+G_{rc}(z)H(z)}\, d(z) \end{aligned} \tag{42}$$

where $G(z)$ is the transfer function from $y_{ref}(z)$ to $y(z)$; $G_d(z)$ is the transfer function from $d(z)$ to $y(z)$; $H(z)$ is the transfer function without plug-in RC, as follows:

$$H(z) = \frac{G_c(z)G_p(z)}{1+G_c(z)G_p(z)} \tag{43}$$

The closed-loop RC control system is asymptotically stable if the following two conditions hold:

(1) The poles of $H(z)$ (i.e. the roots of $1+G_c(z)G_p(z)=0$) are inside the unit circle;

(2) Both the poles of $G(z)$ and $G_d(z)$ (i.e. the roots of $1+G_{rc}(z)H(z)=0$) are inside the unit circle.

For plug-in PSGRC, the condition (2) is also equivalent to the following inequation [14-15]:

$$0 < \sum_{i=0}^{n-1} k_i < 2 \text{ with } k_i \geq 0 \ (i=0,1,2,\ldots, n-1) \tag{44}$$

For plug-in CRC, the condition (2) is equivalent to the following inequation [8]:

$$0 < k_{rc} < 2 \tag{45}$$

Note that both PSGRC and CRC have the same stability range (0, 2) for control gain.

The practical control systems for three-phase and single-phase grid-connected PWM converters are shown in Fig. 9(a) and 9(b), both having the same inner-loop controller and having capability to work in both rectifier and inverter states.

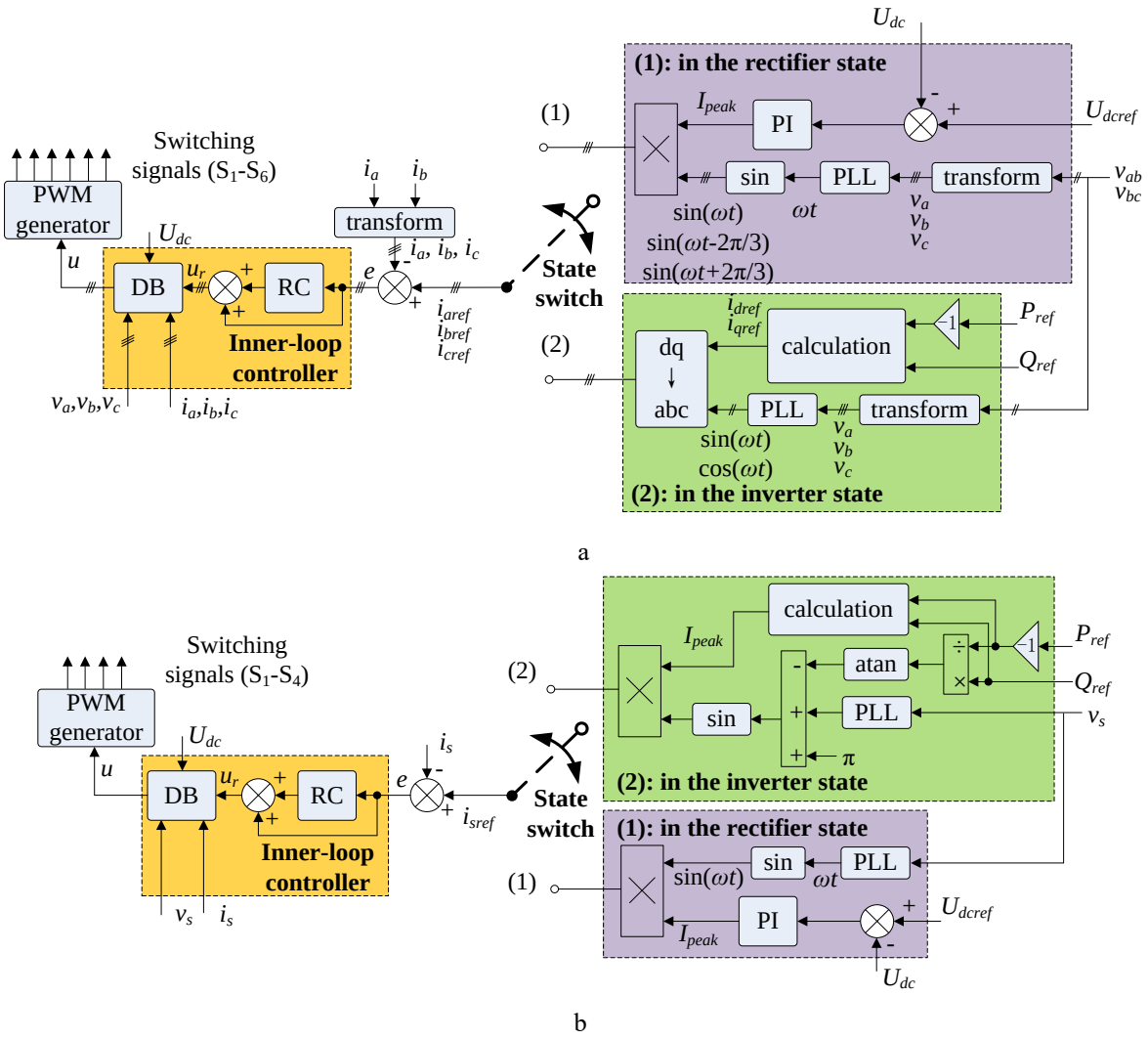

Fig. 9. *Control systems*
a Three-phase
b Single-phase

In the inner-loop control (see *section* 4.3), hybrid controller, including the traditional dead-beat (DB) controller and plug-in RC, i.e. CRC and PSGRC, is used to achieve high accuracy tracking the inductance current reference signal(s), generated by outer-loop controller.

In the outer-loop control, (1) in the rectifier state (dc voltage control outer-loop): PI controller is used to achieve zero-error tracking of the dc voltage reference; (2) in the inverter state (power control outer-loop): instantaneous power theory [18] is used to generate reference current amplitude signal.

4.3. General Inner-loop Controller

The data-sample format of Eq. (30) can be achieved as follows:

$$i_j(k+1)=\frac{b_1-b_2}{b_1}i_j(k)+\frac{1}{b_1}v_j(k)-\frac{c_1}{b_1}U_{dc}(k)u_j(k) \tag{46}$$

where $u_j(k)$ is the duty cycle; j=a,b,c and c_1=1/2 for three-phase and j=s and c_1=1 for single phase; b_1=L/T, b_2=R.

To obtain a uniform and simple controller, both three-phase and single-phase current DB controllers are chosen as:

$$u_j(k)=\frac{2}{U_{dc}(k)}\left[v_j(k)-b_1 i_{jref}(k)+(b_1-b_2)i_j(k)\right] \tag{47}$$

where $i_{jref}(k)=i_j(k+1)$. Thus, the closed-loop transfer function without RC is $H(z)=z^{-1}$. Therefore, the control delay with DB is only one step, i.e. one sample period in theory, which means very fast dynamic response.

In practical applications, RC is usually employed in its digital form, and low-pass filter $Q(z)$ and phase compensator $G_f(z)$ are added to guarantee the stability and robustness of the control system. The plug-in digital CRC and pulg-in digital PSGRC are given as follows

$$G_{\mathrm{CRC}}(z)=k_{rc}\frac{z^{-N}Q(z)}{1-z^{-N}Q(z)}G_f(z) \tag{48}$$

and

$$G_{\mathrm{PSGRC}}(z)=G_f(z)\sum_{i=0}^{n-1}\left[k_i\frac{e^{j(2\pi i/n)}\cdot z^{-N/n}\cdot Q_i(z)}{1-e^{j(2\pi i/n)}\cdot z^{-N/n}\cdot Q_i(z)}\right] \tag{49}$$

where $N=T_o/T_s=f_s/f_o$ with T_s being the system sampling interval and f_s being the system sampling frequency; $G_f(z)$ is the phase lead compensation filter to stabilize the overall closed-loop system; $Q(z)$ and $Q_i(z)$(i = 0, 1, ... , n−1) are low-pass filters (LPFs). In Eq. (48)-(49), N is the time delay steps in the digital CRC controller while N/n is the time delay steps in the digital PSGRC controller. To simplify the design and implementation of phase lead compensator [14], $G_f(z)=z^d$ is usually chosen to compensate the delays in the experimental setup. $Q(z)$ and $Q_i(z)$(i = 0, 1, ... , n−1) are employed to make a good tradeoff between the tracking accuracy and the system robustness with $|Q(e^{j\omega})|\le 1$ and $|Q_i(e^{j\omega})|\le 1$, e.g., $Q(z)=\alpha_1 z+\alpha_0+\alpha_1 z^{-1}$ with $2\alpha_1+\alpha_0=1$, $\alpha_0\ge 0$ and $\alpha_1\ge 0$ [14]. In the experiments, if k_i, the control gain for the i^{th} internal model $G_i(z)$, and k_{n-i}, the control gain of the $(n\text{-}i)^{\mathrm{th}}$ internal model $G_{n-i}(z)$, are same, i.e. $k_i=k_{n-i}$, and $Q_i(z)=Q_{n-i}(z)$, we can get that:

$$k_i G_i(z)+k_{n-i}G_{n-i}(z)=k_i\left[G_i(z)+G_{n-i}(z)\right]$$

$$=k_i\left[\frac{e^{j\left(\frac{i}{n}\cdot 2\pi\right)}\cdot Q_i(z)}{z^{\frac{N}{n}}-e^{j\left(\frac{i}{n}\cdot 2\pi\right)}\cdot Q_i(z)}+\frac{e^{j\left(\frac{-i}{n}\cdot 2\pi\right)}\cdot Q_i(z)}{z^{\frac{N}{n}}-e^{j\left(\frac{-i}{n}\cdot 2\pi\right)}\cdot Q_i(z)}\right]=k_i Q_i(z)\left\{\frac{z^{\frac{N}{n}}2\cos\left(\frac{i}{n}\cdot 2\pi\right)-2Q_i(z)}{z^{\frac{2N}{n}}-z^{\frac{N}{n}}2\cos\left(\frac{i}{n}\cdot 2\pi\right)Q_i(z)+\left[Q_i(z)\right]^2}\right\} \tag{50}$$

where the imaginary parts of complex operators are counteracted if $G_i(z)$ and $G_{n-i}(z)$ have the same control gains and same low-pass filters.

For three-phase grid-connected converter application, let n=6, and corresponding PSGRC (PSGRC-6) can be given:

$$G_{\text{PSGRC-6}}(z)=G_f(z)\sum_{i=0}^{5}\left[k_i\frac{e^{j(\pi i/3)}\cdot z^{-N/6}\cdot Q_i(z)}{1-e^{j(\pi i/3)}\cdot z^{-N/6}\cdot Q_i(z)}\right] \tag{51}$$

For single-phase grid-connected converter application, let n=4, and corresponding PSGRC (PSGRC-4) can be given:

$$G_{\text{PSGRC-4}}(z)=G_f(z)\sum_{i=0}^{3}\left[k_i\frac{e^{j(\pi i/2)}\cdot z^{-N/4}\cdot Q_i(z)}{1-e^{j(\pi i/2)}\cdot z^{-N/4}\cdot Q_i(z)}\right] \tag{52}$$

Another option for single-phase application is letting n=2, and corresponding PSGRC (PSGRC-2, i.e. DMRC [6-7]) can be achieved:

$$G_{\text{PSGRC-2}}(z)=G_f(z)\left[k_0\frac{z^{-N/2}\cdot Q_0(z)}{1-z^{-N/2}\cdot Q_0(z)}-k_1\frac{z^{-N/2}\cdot Q_1(z)}{1+z^{-N/2}\cdot Q_1(z)}\right] \tag{53}$$

5. Experimental Results

5.1. System Parameters

In order to verify the effectiveness and advantages of PSGRC controlled three/single-phase grid-connected converter system, a dSAPCE1104 based PWM IGBT experimental setup is built up. System parameters are shown in Tab I.

By substituting the parameters of Tab. I into Eq. (47), the DB controller can be achieved as follows

$$u_j(k)=\frac{2}{U_{dc}(k)}\left[v_j(k)-30\times i_{jref}(k)+29.5\times i_j(k)\right] \tag{54}$$

where subscript j=a,b,c for three-phase and j=s for single-phase.

Table 1 System parameters

common	only in the rec. state	only in the inv. state
L=5mH	U_{dcref}=120V	P_{ref}=100W (3-P)
R=0.5Ω	k_p=0.5	P_{ref}=50W (1-P)
C=1100μF	k_i=20	Q_{ref}=0
f_s=f_c=6kHz	$v_{ab,\,bc,\,ca,\,s}$ =50V(rms)	$v_{ab,\,bc,\,ca,\,s}$ =25V(rms)
	R_L=60Ω	U_{dc}=50V

For plug-in CRC and PSGRC, major parameters are as follows: (1) phase lead filter $G_f(z)=z^3$ is obtained through practical experimental tests. (2) low-pass filter $Q(z)=0.25z+0.5+0.25z^{-1}$ is chosen for CRC, $Q_i(z)=0.1z+0.8+0.1z^{-1}$ (i=0,1,2,3,4,5) for PSGRC-6, $Q_i(z)=0.1z+0.8+0.1z^{-1}$ (i=0,1,2,3) for PSGRC-4

and $Q_i(z)=0.2z+0.6+0.2z^{-1}$ (i=0,1) for PSGRC-2. (3) k_{rc}=0.2 is chosen for CRC, $k_0=k_2=k_3=k_4=0.05*k_{rc}$, $k_1=k_5=0.4*k_{rc}$ are chosen for PSGRC-6, $k_0=k_2=0.1*k_{rc}$, $k_1=k_3=0.4*k_{rc}$ for PSGRC-4, and $k_0=0.2*k_{rc}$, $k_1=0.8*k_{rc}$ for PSGRC-2. To facilitate the comparison among various RCs, the sum of all control gains are the same, i.e. $k_0+k_1+k_2+k_3+k_4+k_5=k_{rc}=0.2$ for PSGRC-6, $k_0+k_1+k_2+k_3=k_{rc}=0.2$ for PSGRC-4 and $k_0+k_1=k_{rc}=0.2$ for PSGRC-2.

5.2. With only DB Controller

Fig. 10 shows the experimental results with only DB controller for three-phase (3-P) and single-phase (1-P) grid-connected PWM converters in the rectifier (rec.) and inverter (inv.) states.

(a) 3-P in the rectifier state:

Fig. 10(a) shows dc voltage U_{dc} can track its reference value 120V. However, because of the multiple delay factors in the experimental setup, inductance current i_a lags phase voltage v_a by 2~3 sampling periods. That is, i_a still lags phase voltage v_a 2~3 steps.

(b) 3-P in the inverter state:

Fig. 10(b) shows current distortion is relatively serious. That is, current i_a is not a pure sine.

(c) 1-P in the rectifier state:

Fig. 10(c) shows dc voltage U_{dc} can track the reference voltage 120V. However, because of the multiple delay factors, inductance current i_s still lags grid voltage v_s by two sampling periods.

(d) 1-P in the inverter state:

Fig. 10(d) shows current harmonics distortion is relatively serious.

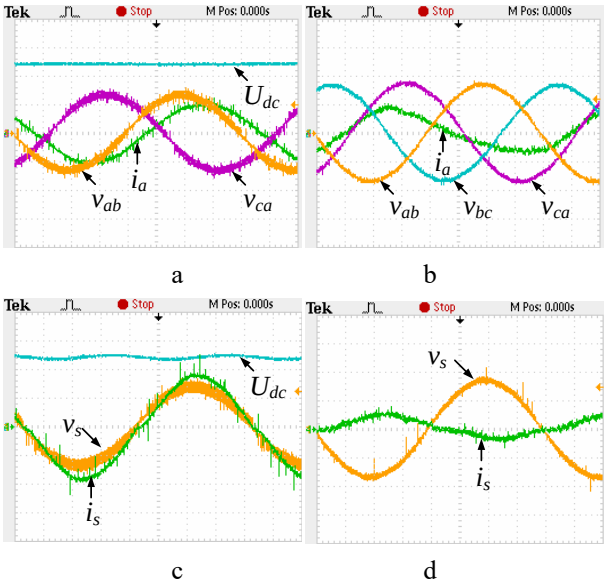

Fig. 10. *Steady-state response with only DB controller (x label: 2.5ms/div, y label: 50V/div & 5A/div for (a)(c) and 20V/div & 2A/div for (b)(d))*
a 3-P in the rectifier state
b 3-P in the inverter state
c 1-P in the rectifier state

d 1-P in the inverter state

5.3. DB+RC

Fig. 11 and Fig. 12 show the steady response and current error tracking histories with CRC and PSGRC plugged into DB for 3-P and 1-P grid-connected converters at rectifier and inverter states.

(a) 3-P in the rectifier state:

Fig. 11(a) shows that, with both plug-in CRC and PSGRC-6, the phase differences between current i_a and voltage v_a in Fig. 10(a) can be compensated, i.e. unit power factor is achieved.

Fig. 12(a) shows that, with both plug-in CRC and PSGRC-6, the current tracking errors are eliminated, i.e. accurate current control is achieved. Moreover, the current error convergence times for CRC and PSGRC-6 are 0.32s and 0.14s, respectively. Therefore, PSGRC-6 can greatly enhance the current error convergence rate, up to three times at most, compared with CRC, i.e. fast current control is achieved.

(b) 3-P in the inverter state:

Fig. 11(b) shows that, with both plug-in CRC and PSGRC-6, the current distortion in Fig. 10(b) can be significantly reduced.

Fig. 12(b) shows that, with both plug-in CRC and PSGRC-6, the tracking errors can be eliminated, i.e. accurate current control is achieved. Moreover, the current error convergence times for CRC and PSGRC-6 are 0.32s and 0.14s, respectively. Therefore, PSGRC-6 can greatly increase the current error convergence rate, up to three times at most, compared with CRC, i.e. fast current control is achieved.

(c) 1-P in the rectifier state:

Fig. 11(c) shows that, with all plug-in CRC, PSGRC-4 and PSGRC-2, the phase differences between current i_s and voltage v_s in Fig. 10(c) can be compensated, i.e. unit power factor is achieved.

Fig. 12(c) shows that, with all plug-in CRC, PSGRC-4 and PSGRC-2, the current tracking errors can be eliminated, i.e. accurate current control is achieved. Moreover, the current error convergence times for CRC, PSGRC-4 and PSGRC-2 are 0.32s, 0.18s and 0.20s, respectively. Therefore, PSGRC-4 and PSGRC-2 can greatly increase the current error convergence rate, up to twice at most, compared with CRC, i.e. fast current control is achieved.

(d) 1-P in the inverter state:

Fig. 11(d) shows that, with all plug-in CRC, PSGRC-4 and PSGRC-2, current distortions in Fig. 10(d) are significantly reduced.

Fig. 12(d) shows that, with all plug-in CRC, PSGRC-4 and PSGRC-2, the current tracking errors can be eliminated, i.e. accurate current control is achieved. Moreover, the current error convergence times for CRC, PSGRC-4 and PSGRC-2 are 0.32s, 0.20s and 0.20s, respectively. Therefore, PSGRC-4 and PSGRC-

2 can greatly increase the current error convergence rate, up to twice at most, compared with CRC, i.e. fast current control is achieved.

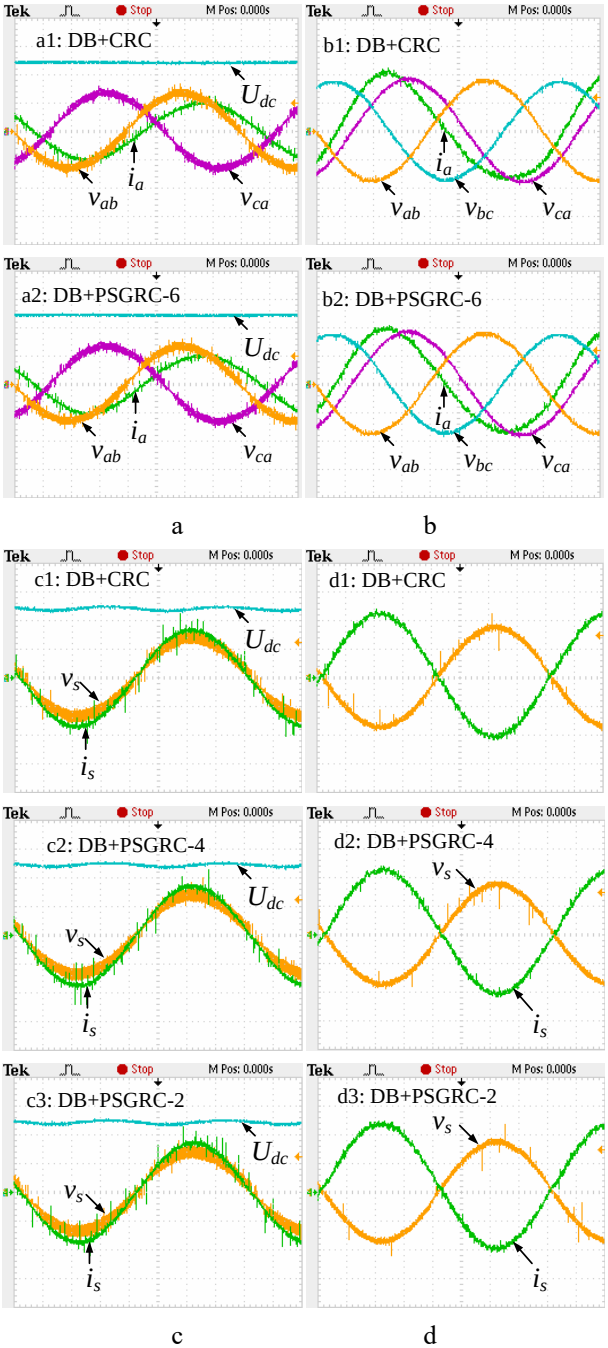

Fig. 11. *Steady-state response with RCs plugged into DB (x label: 2.5ms/div, y label: 50V/div & 5A/div for (a)(c) and 20V/div & 2A/div for (b)(d))*
a 3-P in the rectifier state
b 3-P in the inverter state
c 1-P in the rectifier state
d 1-P in the inverter state

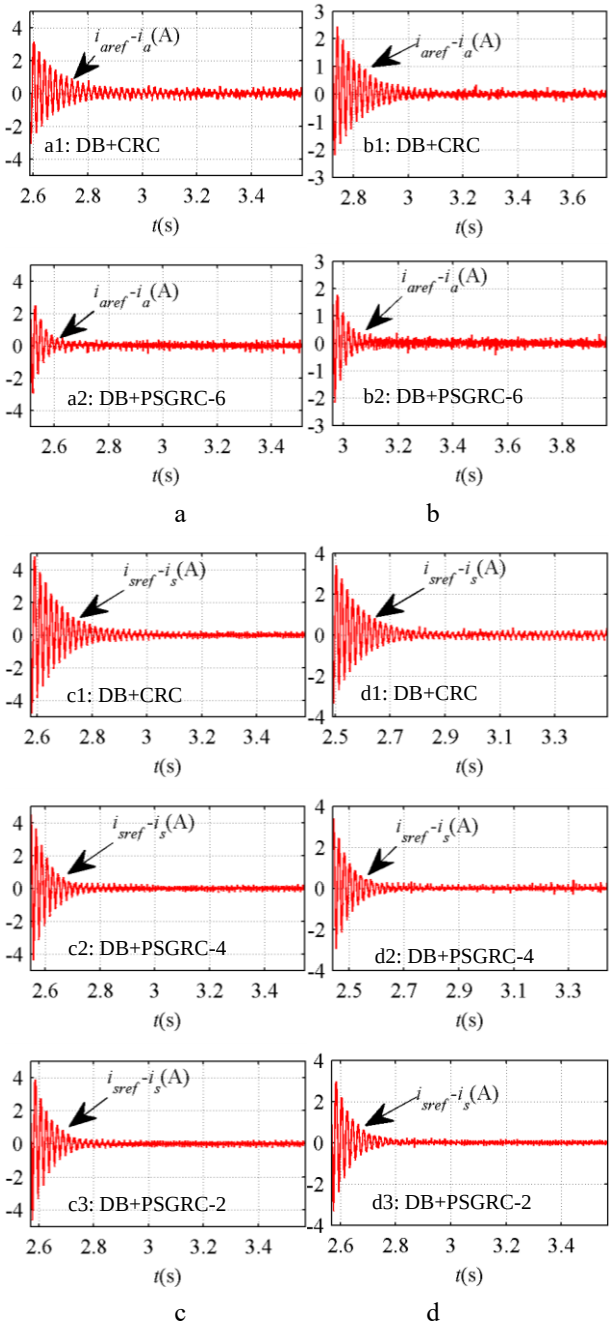

Fig. 12. *Current tracking error histories with RCs plugged into DB*
a 3-P in the rectifier state
b 3-P in the inverter state
c 1-P in the rectifier state
d 1-P in the inverter state

In addition, it should be pointed out that, from above experimental results shown in Fig. 10-12, for the three-phase grid-connected PWM converter systems, both CRC and PSGRC, successfully reduce the current tracking errors from about ±2A to be less than ±0.2A, and force the THDs of the feed-in currents to be about 2%~4%; for the single-phase grid-connected PWM converter systems, both CRC and PSGRC,

successfully reduce the current tracking errors from about ±4A to be less than ±0.2A, and force the THDs of the feed-in currents to be about 1%~2%.

Apparently, both PSGRC and CRC can achieve very high control accuracy. Moreover, by tuning the control gains, PSGRC can achieve faster error convergence rate compared with CRC. PSGRC offers a very effective control scheme for power converters to mitigate power harmonics distortions. Therefore, the effectiveness and advantages of PSGRC for three/single-phase grid-connected PWM converter system are verified.

6. Conclusions

In this paper, parallel structure general repetitive control (PSGRC) is investigated, which includes a series of paralleled $nk+i$ (i=0,1,2,..,n-1) order harmonic internal models. PSGRC can be converted to various RCs for custom demands, such as CRC, DMRC, and so on. PSGRC is applied into general grid-connected PWM converter systems, including three-phase and single-phase converters in the rectifier and inverter states. Experimental results show the effectiveness and advantages of PSGRC. PSGRC controlled three/single-phase grid-connected PWM converter system can achieve the zero-error current tracking and very fast current error convergence rate. Therefore, PSGRC provides a general high performance but low cost control solution to general grid-connected PWM converters.

However, there will be lots of work ahead in the future. Further tests on the proposed PSGRC can be done for many other power converters, such as active power filters with nonlinear load.

7. Acknowledgments

This work was supported in part by the Natural Science Foundation of China under Grant 51407084, by the Fundamental Research Funds for the Central Universities under Grant JUSRP11461, by the Jiangsu Province Science and Technology Support Project under Grant BE2013025.

8. References

[1] Mohan N, Undeland T M. Power electronics: converters, applications, and design[M]. John Wiley & Sons, 2007.
[2] Blaabjerg F, Teodorescu R, Liserre M, et al. Overview of control and grid synchronization for distributed power generation systems[J]. Industrial Electronics, IEEE Transactions on, 2006, 53(5): 1398-1409.
[3] Zhou K, Qiu Z, Watson N R, et al. Mechanism and elimination of harmonic current injection from single-phase grid-connected PWM converters[J]. IET Power Electronics, 2013, 6(1): 88-95.
[4] Francis B A, Wonham W M. The internal model principle of control theory[J]. Automatica, 1976, 12(5): 457-465.
[5] Cosner C, Anwar G, Tomizuka M. Plug in repetitive control for industrial robotic manipulators[C]. IEEE International Conference on Robotics and Automation, Cincinnati, OH, 1990, 1970-1975.
[6] Zhou K, Wang D, Zhang B, et al. Plug-in dual-mode-structure repetitive controller for CVCF PWM inverters[J]. IEEE Transactions on Industrial Electronics, 2009, 56(3): 784-791.
[7] Zhou K, Wang D, Zhang B, et al. Dual-mode structure digital repetitive control[J]. Automatica, 2007, 43(3): 546-554.

[8] Zhou K, Wang D. Digital repetitive controlled three-phase PWM rectifier[J]. IEEE Transactions on Power Electronics, 2003, 18(1): 309-316.
[9] Costa-Castello R, Grino R, Fossas E. Odd-harmonic digital repetitive control of a single-phase current active filter[J]. IEEE Transactions on Power Electronics, 2004, 19(4): 1060-1068.
[10] Escobar G, Hernandez-Briones P G, Martinez P R, et al. A repetitive-based controller for the compensation of 6l±1 harmonic components[J]. IEEE Transactions on Industrial Electronics, 2008, 55(8): 3150-3158.
[11] Zhou K, Low K, Wang D, et al. Zero-phase odd-harmonic repetitive controller for a single-phase PWM inverter[J]. IEEE Transactions on Power Electronics, 2006, 21(1): 193-201.
[12] Lu W, Zhou K, Wang D, et al. A generic digital *nk*±*m* order harmonic repetitive control scheme for PWM converters [J]. IEEE Transactions on Industrial Electronics, 2014, 61(3): 1516-1527.
[13] Lu W, Zhou K, Cheng M, et al. A novel 6*k*±1 order harmonic repetitive control scheme for CVCF three-phase PWM inverters[C]. International Conference on Electrical Machines and Systems, Beijing, 2011, 1-4.
[14] Lu W, Zhou K, Wang D, et al. A general parallel structure repetitive control scheme for multiphase DC-AC PWM converters [J]. IEEE Transactions on Power Electronics, 2013, 28(8): 3980-3987.
[15] Lu W, Zhou K, Wang D. General parallel structure digital repetitive control [J]. International Journal of Control, 2013, 86(1): 70-83.
[16] Gradshteĭn I S, Ryzhik I M, Jeffrey A, et al. Table of Integrals, Series, and Products[M]. 7th ed. San Diego, CA: Academic press, 2007.
[17] Lu W, Zhou K, Yang Y. A general internal model principle based control scheme for CVCF PWM converters[C]. The 2nd IEEE International Symposium on Power Electronics for Distributed Generation Systems, Hefei, 2010, 485-489.
[18] Akagi H, Watanabe E H, Aredes M. Instantaneous power theory and applications to power conditioning[M]. Hoboken: Wiley, 2007.